Longrange surface plasmonpolaritons in asymmetric layer structures

L. Wendler and R. Haupt

Citation: Journal of Applied Physics **59**, 3289 (1986); doi: 10.1063/1.336884
View online: http://dx.doi.org/10.1063/1.336884
View Table of Contents: http://scitation.aip.org/content/aip/journal/jap/59/9?ver=pdfcov
Published by the AIP Publishing

Long-range surface plasmon-polaritons in asymmetric layer structures

L. Wendler and R. Haupt
Sektion Physik der Friedrich-Schiller-Universität Jena, Max-Wien-Platz 1, DDR-6900 Jena, German Democratic Republic

(Received 1 October 1985; accepted for publication 10 December 1985)

We analyze the effect of asymmetric embedding of thin silver layers on the propagation length and the power flow distribution of long-range surface plasmon-polaritons (LRSP). We show that in such configurations LRSP can achieve propagation length which exceeds the value for the symmetric case by up to 3 orders of magnitude.

The recent prediction of long-range surface plasmon-polaritons (LRSP),[1,2] long-range surface phonon-polaritons,[3] and long-range surface plasmon-phonon-polaritons[4] in thin layers has stimulated theoretical[5,6] and experimental[7,8] interest in these new modes. In particular, the application of LRSP to nonlinear optics has received considerable attention. Up to now the investigation of LRSP is based on the demand of surrounding the thin surface-active layer by dielectric media of equal or almost equal[2,9] dielectric constants. However, to date, there has been no systematic investigation of the effect of different dielectric media surrounding the surface-active layer on the properties of LRSP. The purpose of this paper is to investigate the propagation characteristics of LRSP in dependence on the difference of the dielectric constants of the surrounding media.

The system we want to consider is the following. The region $z>a$ is filled by the superstrate with the dielectric constant ϵ_1, the metal layer $a>z>0$ is characterized by a local, homogeneous, isotropic, and frequency-dependent dielectric function $\epsilon_2(\omega)$. The region $0>z$ is filled by the substrate with the dielectric constant ϵ_3. Since the media are isotropic we can specialize on waves propagating in the x direction with the wave vector component $k_\parallel$. These waves must satisfy the following dispersion relation[10]

$$(\epsilon_1\alpha_2+\epsilon_2\alpha_1)(\epsilon_2\alpha_3+\epsilon_3\alpha_2)+(\epsilon_1\alpha_2-\epsilon_2\alpha_1)(\epsilon_2\alpha_3-\epsilon_3\alpha_2)e^{-2\alpha_2 a}=0\,, \tag{1}$$

with

$$\alpha_i=\left(k_\parallel^2-\epsilon_i(\omega)\frac{\omega^2}{c^2}\right)^{1/2}. \tag{2}$$

For our calculations we have chosen Ag layers with $\epsilon_2=-18+i0.47$ at the He-Ne laser wavelength[11] $\lambda=632.8$ nm and for the fixed values of the dielectric constants ϵ_1 or ϵ_3 we have used 2.1211 (fused silica). In the numerical analysis we assume a complex wave vector component $k_\parallel$ and a real frequency ω that is related to an angle-scan ATR (attenuated total reflection) experiment. The propagation length L of LRSP is then given by

$$L=\frac{1}{2|\mathrm{Im}\,k_\parallel|}. \tag{3}$$

For a variation of the system parameters described above, three physically different possibilities exist:

(a) The metal layer thickness a and the dielectric constant ϵ_3 of the substrate are fixed and the dielectric constant ϵ_1 of the superstrate is altered to lower values.

(b) The metal layer thickness a and the dielectric constant ϵ_1 of the superstrate are fixed and the dielectric constant ϵ_3 of the substrate is altered to higher values.

(c) The dielectric constants ϵ_1 and ϵ_3 are fixed and the thickness of the surface-active metal layer is varied.

In all cases we have chosen $\epsilon_1\lesssim\epsilon_3$ with respect to ATR experiments and without loss of generality. The variation of the parameters has two physical effects on LRSP: (i) an increasing or decreasing of the velocity of the energy flow of LRSP and (ii) a changing of the power flow distribution of LRSP (superstrate ↔ metal layer ↔ substrate). In Fig. 1 these processes are demonstrated. Figure 1(a) shows the dispersion relation of LRSP for a symmetric configuration ($\epsilon_1=\epsilon_3$) and Figs. 1(b)–1(d) for asymmetric configurations. From these figures can be seen that in the asymmetric case a natural *stop point* exists for the occurrence of LRSP.

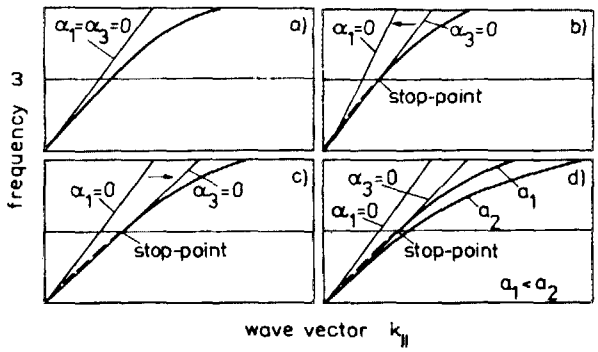

FIG. 1. Dispersion relation of LRSP: (a) symmetric configuration, (b)–(d) asymmetric configurations. (b) Fixed: layer thickness a and dielectric constant ϵ_3 of the substrate, dielectric constant ϵ_1 of the superstrate is altered to lower values, (c) fixed: layer thickness a and dielectric constant ϵ_1, dielectric constant ϵ_3 is altered to higher values, (d) fixed: dielectric constants ϵ_1 and ϵ_3, the thickness a of the layer is varied.

 0021-8979/86/093289-03$02.40

This stop point is given by Eq. (1) with $\alpha_3 = 0$

$$\frac{\epsilon_2}{\epsilon_1}\left(\frac{\epsilon_3-\epsilon_1}{\epsilon_3-\epsilon_2}\right)^{1/2} + \tanh\left(\frac{\omega}{c}a(\epsilon_3-\epsilon_2)^{1/2}\right) = 0 . \quad (4)$$

In case (a) [Fig. 1(b)] the velocity of the energy flow of LRSP increases in comparison to that of LRSP occurring in a symmetric embedded Ag layer, whereas the velocity of the energy flow is decreasing in case (b) [Fig. 1(c)]. The power flow distribution in an asymmetric configuration is quite different from that in a symmetric one. In Table I the calculated power flow and the propagation length of LRSP are given for a Ag layer of the thickness $a = 17$ nm. As can be seen from the table, the power flow in the substrate is increasing at the expense of that in the superstrate and in the Ag layer. As a consequence of this power flow redistribution towards lower values in the Ag layer, the propagation length of LRSP increases sharply.

Figure 2 shows the numerical results of the propagation length of LRSP in dependence on the dielectric constants ϵ_1 and ϵ_3 for various thicknesses of the Ag layer. The left part of the curves in Fig. 2 corresponds to case (a) (ϵ_3 is fixed, ϵ_1 is varying) and the right part of the curves corresponds to case (b) (ϵ_1 is fixed, ϵ_3 varies). Both parts of each curve are not symmetrical to each other. The different velocities of the energy flow in case (a) and (b) [cf. Fig. 1(b) and 1(c)] are the reason for this behavior. From Fig. 2 is to be seen that in the near of the stop point of LRSP a *critical range* of the difference $\Delta\epsilon$ between ϵ_1 and ϵ_3 exists where the propagation length increases sharply (see also Table I).

For thick Ag layers ($a \geqslant 30$ nm) the propagation length shows a plain maximum in the range $\epsilon_1 \approx \epsilon_3$ before it increases in dependence on $\Delta\epsilon$. The growth in the propagation length that can be attained in the critical range of $\Delta\epsilon$ in comparison to that for $\epsilon_1 \approx \epsilon_3$ is small. However, important for thick Ag layers is that LRSP can exist in a wide range of $\Delta\epsilon$ without dramatic change of the propagation length of LRSP. If the thickness of the Ag layer is decreased, the maximum of L in the range $\epsilon_1 \approx \epsilon_3$ disappears, and the curves are narrowed. In this case, the range of $\Delta\epsilon$ where LRSP can exist at all is very small, but the growth in the propagation length near the stop points is enormous. For thin Ag layers ($a \leqslant 20$ nm) the propagation length that can be attained in the critical range exceeds the values for $\epsilon_1 \approx \epsilon_3$ by up to 3 orders of magnitude (see Fig. 2 and Table I). The consequence for experimental work is to find out an optimum layer thickness taking into account both effects described above.

TABLE I. Propagation length (L) and power flow in the superstrate (P_1), in the Ag layer (P_2), and in the substrate (P_3) for various combinations of the dielectric constants ϵ_1 and ϵ_3 of the superstrate and the substrate, respectively. The data are taken at the He-Ne wavelength for a Ag layer of the thickness $a = 17$ nm.

ϵ_1	ϵ_3	L	P_1	P_2	P_3
2.0188	2.1211	1.9824 cm	0.778%	0.007%	99.215%
2.0198	2.1211	0.5010 cm	2.255%	0.019%	97.725%
2.1211	2.1211	0.0515 cm	49.830%	0.340%	49.830%
2.1211	2.2340	0.4992 cm	2.004%	0.019%	97.977%
2.1211	2.2352	1.9854 cm	0.466%	0.004%	99.530%

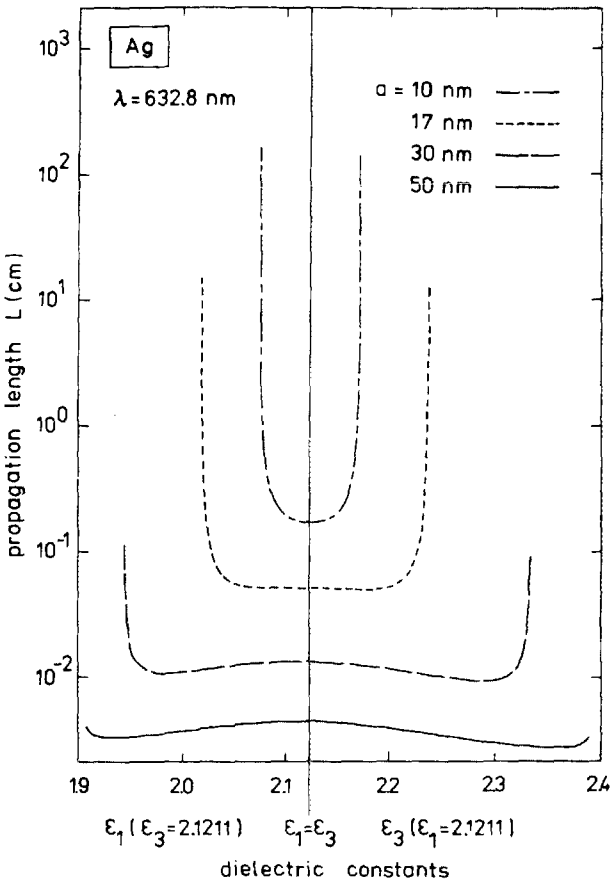

FIG. 2. Propagation length of LRSP vs dielectric constants ϵ_1 of the superstrate and ϵ_3 of the substrate for different thicknesses a of the Ag layer.

In Fig. 3 the propagation length of LRSP is plotted in dependence on the thickness a of the Ag layer for various combinations of the dielectric constants of the surrounding media [case (c)]. The propagation length increases with

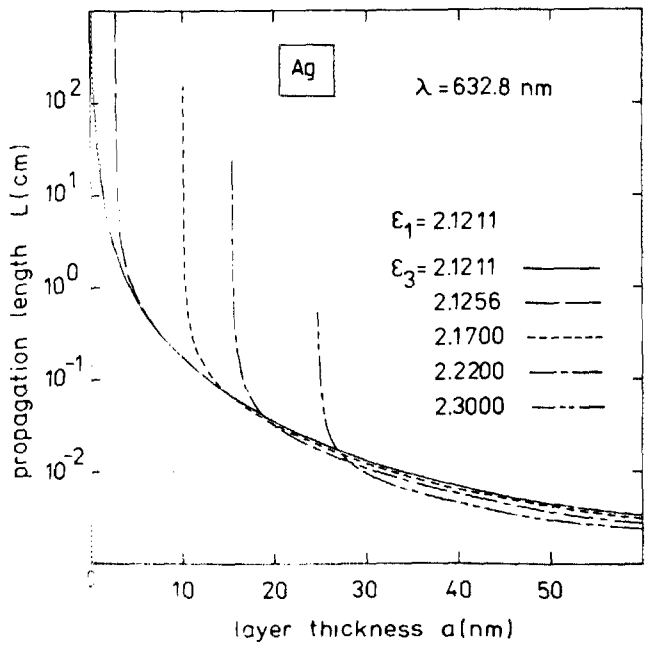

FIG. 3. Propagation length of LRSP vs thickness a of the Ag layer for various dielectric constants ϵ_3 of the substrate.

decreasing thickness of the Ag layer. This is well known from symmetric embedded surface-active Ag layers. In the case of a finite difference of the dielectric constants ϵ_1 and ϵ_3 the propagation length of LRSP is limited by the stop point given in Eq. (4). However, for a given thickness a of the Ag layer a considerable increase of the propagation length can be attained using a suitable $\Delta\epsilon$, so that the critical range of the propagation length falls in the range of the chosen layer thickness a. This is an important fact for the experimental work, because the preparation of homogeneous Ag layers less than 10 nm thick is difficult and often results in an island structure.

In the following we give so-called *design parameters* which allow the estimation of one of the parameters in the critical range near the stop point of LRSP in dependence on the other parameters. The knowledge of these design parameters is very useful for the fabrication of suitable LRSP guiding systems, because it is possible to check the parameter range where LRSP can exist in a chosen configuration.

We obtain the following design parameters in the nearness of the stop point. For large layer thicknesses and given values of ϵ_2 and ϵ_3 the dielectric constant of the superstrate is

$$\epsilon_1 = \frac{\epsilon_2'^2}{2(\epsilon_3 - \epsilon_2')}\left[\left(1 + \frac{4\epsilon_3(\epsilon_3 - \epsilon_2')}{\epsilon_2'^2}\right)^{1/2} - 1\right] \quad (5)$$

and for given values of ϵ_1 and ϵ_2 the dielectric constant of the substrate is

$$\epsilon_3 = \frac{\epsilon_1\epsilon_2'}{\epsilon_1 + \epsilon_2'}. \quad (6)$$

ϵ_2' is the real part of ϵ_2. If the Ag layers are very thin the design parameters are

$$\epsilon_1 = \frac{\epsilon_2'^2}{2(\epsilon_3 - \epsilon_2')^2}\frac{c^2}{\omega^2 a^2} \times\left[\left(1 + \frac{4\epsilon_3(\epsilon_3 - \epsilon_2')^2}{\epsilon_2'^2}\frac{\omega^2 a^2}{c^2}\right)^{1/2} - 1\right] \quad (7)$$

and

$$\epsilon_3 = \left(\frac{\epsilon_2'^2}{2\epsilon_1^2}\frac{c^2}{\omega^2 a^2} + \epsilon_2'\right) \times\left[1 - \left(1 - \frac{4\epsilon_1^3\omega^2 a^2(c^2 + \epsilon_1\omega^2 a^2)}{(\epsilon_2' c^2 + 2\epsilon_1^2\omega^2 a^2)^2}\right)^{1/2}\right]. \quad (8)$$

For given dielectric constants ϵ_1, ϵ_2, and ϵ_3, the design value of the layer thickness a for working in the nearness of the stop point is

$$a = -\frac{c}{\omega}\frac{\epsilon_2'}{\epsilon_1(\epsilon_3 - \epsilon_2')}(\epsilon_3 - \epsilon_1)^{1/2}. \quad (9)$$

The main result of this communication is that the propagation length of LRSP can be highly increased up to 3 orders of magnitude using suitable values of the difference between the dielectric constant ϵ_1 of the superstrate and the dielectric constant ϵ_3 of the substrate for a given thickness of the Ag layer. Working in such a regime results for example in enhanced nonlinear effects, because first, the propagation length of LRSP is sharply increased and second, their power flow is enhanced in the substrate which is the nonlinear medium in those experiments.

[1] M. Fukui, V. C. Y. So, and R. Normandin, Phys. Status Solidi B **91**, K61 (1979).
[2] D. Sarid, Phys. Rev. Lett. **47**, 1927 (1981).
[3] Z. Lenac and M. S. Tomaš, J. Phys. C **16**, 4273 (1983).
[4] L. Wendler and R. Haupt, J. Phys. C (in press).
[5] G. I. Stegeman, J. J. Burke, and D. G. Hall, Appl. Phys. Lett. **41**, 906 (1982).
[6] R. T. Deck and D. Sarid, J. Opt. Soc. Am. **72**, 1613 (1982).
[7] J. C. Quail, J. G. Rako, and H. J. Simon, Opt. Lett. **8**, 377 (1983).
[8] J. C. Quail, J. G. Rako, H. J. Simon, and R. T. Deck, Phys. Rev. Lett. **50**, 1987 (1983).
[9] H. Dohi, Y. Kuwamura, M. Fukui, and O. Tada, J. Phys. Soc. Jpn. **53**, 2828 (1984).
[10] L. Wendler, Phys. Status Solidi B **123**, 469 (1984).
[11] P. B. Johnson and R. W. Christy, Phys. Rev. B **12**, 4370 (1972).

Hugoniot measurements for vanadium

G. Roger Gathers
University of California, Lawrence Livermore National Laboratory, Livermore, California 94550

(Received 5 August 1985; accepted for publication 14 January 1986)

The Hugoniot of vanadium has been measured by means of a two-stage light-gas gun which launches planar impactors at velocities up to 8 km/s. The data fit the relation $U_s = C + S\,U_p$, where U_s is shock velocity, U_p is particle velocity, $C = 5.044$ km/s, and $S = 1.242$ in the pressure range 20–337 GPa.

Considerable advances in the precision of shock-wave measurements and increases in the useful velocities available from gas guns have occurred[1,2] since much of the Hugoniot data in the literature were measured.[3–6] The work described here was undertaken to improve the data base with new measurements and to investigate features reported previously for vanadium and other transition metals. For example, Al'tshuler *et al.* reported a slope change in the shock velocity-particle velocity relationship for vanadium.[4] This result could not be tested by plane-wave explosive systems,[3,5] which launch planar impactors to a maximum velocity of 5 km/s. Our two-stage light-gas gun launches impactors up to 8 km/s and can probe the full pressure range of the Soviet vanadium data.

0021-8979/86/093291-03$02.40